Trim for Maximum Control Authority using the Attainable Moment Set

Varriale, Carmine; Veldhuis, Leo; Voskuijl, Mark

DOI
10.2514/6.2020-1265

Publication date
2020

Document Version
Final published version

Published in
AIAA Scitech 2020 Forum

AIAA SciTech Forum
6-10 January 2020, Orlando, FL
AIAA Scitech 2020 Forum

10.2514/6.2020-1265

Trim for Maximum Control Authority using the Attainable Moment Set

Carmine Varriale*
Delft University of Technology, Delft, 2629 HS, The Netherlands

Mark Voskuijl†
Netherlands Defence Academy, Den Helder, 1780 AC, The Netherlands

Leo L. M. Veldhuis‡
Delft University of Technology, Delft, 2629 HS, The Netherlands

This paper presents a method to find trimmed flight conditions while maximizing the available control authority about one or more motion axes. Maximum pitch-up, or lift-up, control authority could find interesting application in aborted landing situations, while maximum balanced control authority about all motion axes is a reformulation of the classic concept of minimum control effort. The trim problem is formulated in the form of a constrained optimization problem. The constraints and the objective function are obtained by exploiting the geometric properties of the Attainable Moment Set, a convex polytope containing the forces and moments attainable by the aircraft control effectors. The method is applied to an innovative box-wing aircraft configuration called PrandtlPlane, whose double wing system can accommodate a large number of control surfaces, and hence allow Pure Torque and Direct Lift Control possibilities. Control surface deflections are compared for trim conditions with maximum control authority in the pitch axis, in the lift axis, and maximum balanced control authority, for symmetric and asymmetric flight. Results show that the method is able to capitalize on the angle of attack or the throttle setting to obtain the control surfaces deflections which maximize control authority in the assigned direction.

Nomenclature

α, β, γ	angles of attack, side-slip, flight path, rad
ϕ, θ, ψ	angles of bank, elevation, heading, rad
$\boldsymbol{\delta}$	effector positions, rad
$\boldsymbol{\mathcal{X}}$	trim controls set
g	gravitational acceleration, $\mathrm{m\cdot s^{-2}}$
ℓ	half-line in Moment Space
p, q, r	angular rates in Body Axes, $\mathrm{rad\cdot s^{-1}}$
u, v, w	velocity components in Body Axes, $\mathrm{m\cdot s^{-1}}$
$\boldsymbol{f}$	equations of motion
$\boldsymbol{u}, \boldsymbol{x}$	dynamic system inputs and states
B	control effectiveness matrix, $\mathrm{rad^{-1}}$
$C_{(\,)}$	generic non-dimensional coefficient
I	inertia tensor, $\mathrm{kg\cdot m^2}$
L	lift force, N
M_∞	free-stream Mach number
V	airspeed, $\mathrm{m\cdot s^{-1}}$
W	aircraft weight, N
$X_\mathrm{A}, Y_\mathrm{A}, Z_\mathrm{A}$	forces in Aerodynamic Axes, N
$X_\mathrm{B}, Y_\mathrm{B}, Z_\mathrm{B}$	forces in Body Axes, N
$X_\mathrm{E}, Y_\mathrm{E}, Z_\mathrm{E}$	aircraft position in Earth Axes, m
$\boldsymbol{F}$	generalized forces, N or N·m
$\mathcal{A}$	control authority
$\mathcal{J}$	generic objective function
$\mathcal{L}_\mathrm{A}, \mathcal{M}_\mathrm{A}, \mathcal{N}_\mathrm{A}$	moments in Aerodynamic Axes, N·m
$\mathcal{L}_\mathrm{B}, \mathcal{M}_\mathrm{B}, \mathcal{N}_\mathrm{B}$	moments in Body Axes, N·m

Subscripts and superscripts

a, e, r	aileron, elevator, rudder
dyn, kyn	dynamic, kynematic
ineq, *eq*	inequality, equality constraint
lb, ub	lower bound, upper bound
T	thrust
tr	trim condition
w, h, c	wing, horizontal tail, canard
$\mathcal{A}$	aerodynamic effect

Acronyms and abbreviations

AMS	Attainable Moment Set
CH	Convex Hull
DoF	Degree of Freedom
GAMS	Greatest Attainable Moment Set
SW	side wind

*Ph.D. Candidate, Flight Performance and Propulsion Section, Faculty of Aerospace Engineering, C.Varriale@tudelft.nl; AIAA Member.
†Full Professor, Faculty of Military Sciences, M.Voskuijl@mindef.nl; AIAA Member.
‡Full Professor, Flight Performance and Propulsion Section, Faculty of Aerospace Engineering; AIAA Member.

Fig. 1 Three Northrop Grumman F2F-1 fighters in formation flight, 1939*.

I. Introduction

Trimming a dynamic system means finding the combination of input and state variables values which set the system in a steady-state condition [1]. The latter can be representative of either a static or dynamic equilibrium condition. In the most general case, the dynamic system is represented in the state-space form by non-linear, implicit or explicit equations. Respectively:

$$\boldsymbol{f}\left(\dot{\boldsymbol{x}},\ \boldsymbol{x},\ \boldsymbol{u}\right) = \boldsymbol{0} \quad \text{or} \quad \dot{\boldsymbol{x}} = \boldsymbol{f}\left(\boldsymbol{x},\ \boldsymbol{u}\right). \tag{1}$$

If the system is trimmed, then

$$\boldsymbol{f}\left(\dot{\boldsymbol{x}}^{\text{tr}} = \boldsymbol{0},\ \boldsymbol{x}^{\text{tr}},\ \boldsymbol{u}^{\text{tr}}\right) = \boldsymbol{0} \quad \text{or} \quad \dot{\boldsymbol{x}}^{\text{tr}} = \boldsymbol{f}\left(\boldsymbol{x}^{\text{tr}},\ \boldsymbol{u}^{\text{tr}}\right) = \boldsymbol{0}. \tag{2}$$

The trim problem is the problem of finding the values of $\boldsymbol{x}^{\text{tr}}$ and $\boldsymbol{u}^{\text{tr}}$ such that Eq. 2 is verified.

Let us indicate with $\mathbb{X} = \{\boldsymbol{x}, \boldsymbol{u}\}$ the set of system states and inputs. For a given trim condition, $\mathbb{X}^{\text{tr}} = \left\{\boldsymbol{x}^{\text{tr}}, \boldsymbol{u}^{\text{tr}}\right\}$. In general, some subset $\boldsymbol{\mathcal{X}}_0 \subseteq \mathbb{X}$ can (or must) be characterized explicitly in order to define the desired trim condition. The variables belonging to this subset have therefore known values. The remaining subset $\boldsymbol{\mathcal{X}} = \mathbb{X} - \boldsymbol{\mathcal{X}}_0$ contains unknown valued variables, which are referred to as *trim controls*. By using these definitions, it is possible to represent $\mathbb{X}^{\text{tr}}$ either in terms of system states and inputs or in terms of assigned and unknown trim parameters:

$$\mathbb{X}^{\text{tr}} = \left\{\boldsymbol{x}^{\text{tr}},\ \boldsymbol{u}^{\text{tr}}\right\} = \{\boldsymbol{\mathcal{X}}_0,\ \boldsymbol{\mathcal{X}}\}. \tag{3}$$

The trim problem consists then in determining the values of the trim controls $\boldsymbol{\mathcal{X}}$ that verify Eq. 2.

We can indicate with $N_{\boldsymbol{f}}$ the number of dynamic equations $\boldsymbol{f}$, and with $N_{\boldsymbol{\mathcal{X}}}$ the number of trim controls $\boldsymbol{\mathcal{X}}$. The trim problem is said to be over-determined if $N_{\boldsymbol{f}} > N_{\boldsymbol{\mathcal{X}}}$, determined if $N_{\boldsymbol{f}} = N_{\boldsymbol{\mathcal{X}}}$, or under-determined if $N_{\boldsymbol{f}} < N_{\boldsymbol{\mathcal{X}}}$. This classification does not give any indication on the number of solutions that the trim problem can have. Due to non-linearities and couplings in the dynamics equations, even a determined trim problem can have zero or more than one solution: an example of this is shown in Fig. 1. In the figure, the leader is trimmed in straight and level flight. The followers are trimmed in an anti-symmetric, steady forward-slip flight. This attitude requires additional contemporary deflection of ailerons and rudders to maintain the asymmetric flight condition. The additional trim drag requires in turn a higher engine setting to maintain a horizontal trajectory. The complexity of a given trim problem increases with the number of trim controls, making under-determined problems generally tougher to solve than determined ones.

For aircraft flight mechanics applications, a common choice for the state vector $\boldsymbol{x}$ is:

$$\boldsymbol{x} = \left[\boldsymbol{x}_{\text{dyn}},\ \boldsymbol{x}_{\text{kyn}}\right] \qquad \text{with} \quad \boldsymbol{x}_{\text{dyn}} = [u, v, w, p, q, r], \quad \boldsymbol{x}_{\text{kyn}} = [\psi, \theta, \phi, X_{\text{E}}, Y_{\text{E}}, Z_{\text{E}}]. \tag{4}$$

*Courtesy of the National Archives and Records Administration; catalog number: 80-G-409231.

where ψ, X_E and Z_E have no influence on dynamics (in case of non geo-referenced applications), and Z_E is only used for retrieving the properties of the atmosphere at the current altitude. Alternatively, the velocity components in Body Axes $[u, v, w]$ are sometimes replaced by airspeed and aerodynamic angles $[V, \alpha, \beta]$. Also, the Euler angles $[\psi, \theta, \phi]$ are often replaced by the attitude quaternion, in order to avoid the "gimbal lock" phenomenon [2].

An extensive and detailed analysis of the trim problem for rigid aircraft 6-DoF dynamics is presented in [3]. A remarkable effort is devoted to a unified analytical derivation of the equations of motion and to the formulation of the trim problem for typical flight conditions. In all cases, a conventional aircraft configuration is considered, with four input variables related to the four classic control effectors (throttle position, and elevator, aileron and rudder deflections). The two ailerons are considered ganged, i.e. their deflections are linked through a fixed gearing ratio. The same is done with the elevators, if more than one is present. Hence, each of these pairs of control surfaces represents only one input variable for the aircraft dynamic system:

$$\boldsymbol{u} = [\delta_T,\ \delta_e,\ \delta_a,\ \delta_r]. \tag{5}$$

The trim problem is formulated as the following optimization problem:

$$\begin{aligned} \min_{\boldsymbol{\mathcal{X}}} \quad & \mathcal{J} = \left\| \dot{\boldsymbol{x}}_{dyn} \right\|^2 \\ \text{subj. to} \quad & \boldsymbol{\mathcal{X}}_{lb} \leq \boldsymbol{\mathcal{X}} \leq \boldsymbol{\mathcal{X}}_{ub} \end{aligned} \tag{6}$$

and assumes the aircraft is trimmed when the non-negative objective function $\mathcal{J}$ approaches 0 within a certain tolerance. The problem is then, in essence, a root finding problem. For every desired flight condition the number of assigned trim parameters $\boldsymbol{\mathcal{X}}_0$ is chosen so that the trim problem is determined. Since a dynamic model based on the 6-DoF rigid-body equations of motion is adopted, each trim problem has six trim controls: the four input parameters of Eq. 5, plus two Euler angles. This approach shows its limitations when considering aircraft configurations with higher number of inputs, e.g. with redundant or unganged sets of control effectors, for which the trim problem becomes under-determined.

An early attempt at solving an under-determined trim problem for aircraft longitudinal dynamics is provided in [4]. The trim problem is formulated as an induced drag minimization problem, with constraints on the vertical and rotational equilibrium in the longitudinal axis. The equations of motion are linearized with classic assumptions for the cruise condition and a closed form solution is derived. Examples are provided for a three-lifting surface-aircraft and a fighter jet with thrust vectoring capabilities. The trim controls $\boldsymbol{\mathcal{X}}$ for the first system are the lifts of each surface, while those for the second case are the lifts of wing and tail, and the engines' thrust angle. In both cases, $N_{\boldsymbol{\mathcal{X}}} = N_{\boldsymbol{f}} + 1$ and therefore it is possible to optimize a single scalar parameter, induced drag, while trimming the aircraft.

The case of under-determined trim problems due to control effectors redundancy has been analyzed in [5], with application to the Blended Wing Body (BWB) aircraft configuration. Two approaches to the trim problem are proposed:

1) A Minimum Drag Trim Optimization (MDTO) formulation applied to 6-DoF dynamics.
2) A Trim Direct Allocation (TDA) formulation, analogous to the one in Eq. 6.

With the MDTO formulation, the trim controls $\boldsymbol{\mathcal{X}}$ directly include unganged control surfaces deflections $\boldsymbol{\delta}$. In this way, the dimension of $\boldsymbol{\mathcal{X}}$ increases linearly with the amount of control effectors, making the trim problem more complex for highly-redundant aircraft configurations.

With the TDA formulation, the unknown control surfaces deflections $\boldsymbol{\delta}$ are replaced, in the trim control subset $\boldsymbol{\mathcal{X}}$, by a set of unknown aerodynamic actions due to the control effectors $\Delta\boldsymbol{F}$. A Direct Control Allocation (DCA) method f_{CA}, as developed in [6], is used to establish a relation between $\Delta\boldsymbol{F}$ and the control surfaces deflections $\boldsymbol{\delta}$, through the control effectiveness matrix $\boldsymbol{B}$:

$$\Delta\boldsymbol{F} = \boldsymbol{B}\boldsymbol{\delta} \quad \Rightarrow \quad \boldsymbol{\delta} = f_{CA}(\boldsymbol{B})\,\Delta\boldsymbol{F}. \tag{7}$$

With this approach, the dimension of $\boldsymbol{\mathcal{X}}$ does not depend on the control redundancy of the aircraft configuration. The dimension of $\Delta\boldsymbol{F}$, here indicated with $N_{\boldsymbol{F}}$, is somewhat arbitrary and depends on which motion axes are selected to be controlled: $\Delta\boldsymbol{F}$ contains up to two elements (lift and pitch moment) for flight simulations constrained in the longitudinal plane, or up to four elements (lift, and roll, pitch, yaw moments) for 6-DoF simulations. It is noted that the number and type of elements in $\Delta\boldsymbol{F}$ has a significant impact on the control surfaces deflections at trim $\boldsymbol{\delta}^{tr}$.

Comparing the two approaches presented in [5] would be overall unfair. The MDTO is an optimization-based approach that exploits controls redundancy to minimize drag at trim conditions. The TDA is a root-finding trim approach that copes with control redundancy through a neutral objective Control Allocation (CA) algorithm. No parameter is explicitly optimized with the latter formulation and indeed the method is not capable of returning the minimum drag trim condition. With reference to the TDA approach, it is shown that introducing lift in the trim control vector results in

Table 2 Summary of trim problem formulations from the reviewed literature.

Reference	DoF	Objective	Trim Controls	Control Surfaces Gearing
[3]	6	Trim	θ, ψ, δ_{T}, δ_{e}, δ_{a}, δ_{r}	Ganging
[4]	3	Drag	$C_{L,\mathrm{w}}$, $C_{L,\mathrm{h}}$, $C_{L,\mathrm{c}}$	Not modeled
	3	Drag	$C_{L,\mathrm{w}}$, $C_{L,\mathrm{h}}$, δ_{T}	Not modeled
[5]	3,6	Trim, drag	α, θ, $\boldsymbol{\delta}$, δ_{T}	None
	3	Trim	α, θ, $\mathcal{M}$, δ_{T}	DCA [6]
	3	Trim	α, θ, $\mathcal{M}$, Z_{B}, δ_{T}	DCA [6]
	6	Trim	α, θ, ψ, ϕ, $\mathcal{L}$, $\mathcal{M}$, $\mathcal{N}$, Z_{B}, δ_{T}	DCA [6]

trim conditions with better aerodynamic efficiency, i.e. lower drag. Drag is not explicitly included in $\mathcal{X}$ because the DCA would poorly approximate its quadratic behavior with deflection angles.

Advanced CA algorithms that explicitly minimize drag have been developed in the past, but never applied to the trim problem. For example, an incremental, or frame-wise, expansion of the DCA method is presented in [7]. Alternatively, a model-specific incremental CA method is presented in [8], where drag is expressed as a quadratic function of the effectors, and the CA algorithm solves a quadratic programming optimization problem.

A synthetic scheme of the reviewed trim problem formulations is shown in Table 2.

This paper presents a trim problem formulation aimed at achieving maximum control authority in a specific direction of one or more motion axes. The trim problem is formulated in the form of a constrained optimization problem. The constraints and the objective function are obtained by exploiting the geometric properties of the Attainable Moment Set (AMS), a convex polytope representing all the possible forces and moments attainable by the aircraft control effectors. Forces and moments are then mapped to the effectors using a Linear Programming formulation of the DCA method.

Control authority is here defined as the ability of the control effectors to generate forces and moments in the given direction of the selected set of motion axes. For example, maximizing balanced control authority about all motion axes can be interpreted as a reformulation of the classic problem of minimizing total control effort.

The condition in which an aircraft is flying in equilibrium but is capable of generating maximum pitch-up control moment could be of interest for an aborted landing situation. In such a flight scenario, due to high lift devices introducing a consistent additional pitch-down moment, conventional aircraft configurations need to deploy a significant pitch-up elevator deflection just to trim the aircraft. The greater the trim deflection demanded to the elevator for trim, the smaller the control authority left for emergency pitch-up maneuvers. Searching for trim conditions which guarantee rotational equilibrium and at the same time increase the control authority for pitch-up is therefore interesting with regards to safety purposes. A similar scenario can be envisioned to justify the interest in trim with maximum lift-up control authority. Because lift lies perpendicular to the velocity vector, by definition, an increase in lift introduces a centripetal acceleration $V\dot{\gamma}$ which is the most direct way to bend the trajectory upwards. The study of control authority in the lift axis is particularly aimed at exploiting one of the most interesting capabilities of the box-wing aircraft configuration: the innovative way of implementing Direct Lift Control (DLC). With the redundant controls on the double wing system, box-wings are capable of generating substantial variation in lift, while decoupling, partially or totally, the control of pitch moment from the one of vertical forces.

The aircraft flight mechanics and simulation model used is presented in Sec. II. The concept of control authority is formalized in the scope of CA theory in Sec. III, and the new trim problem formulation is illustrated in Sec. IV. Applications to 3-DoF simulations are presented for explanatory purposes. Results for 6-DoF simulations are shown in Sec. V for maximum control authority in the pitch and lift axes, as well as for maximum balanced control authority about all motion axes. Finally, conclusions and further studies are presented in Sec. VI.

II. Aircraft and Simulation Model

The concepts developed in this work apply to any aircraft configuration, with any level of control redundancy. The aircraft model used as the main application case for this paper is an unconventional, box-wing configuration referred to as the PrandtlPlane (PrP). The specific PrP used for this study is a 300 passenger, transonic, commercial transport aircraft, currently being designed within the scope of the PARSIFAL project [9, 10], in the framework of the European

Horizon 2020 research program. The box-wing has been known for a long time to be the "best wing system" for induced drag performance [11], and the PrP concept strives to integrate it in an innovative aircraft architecture for sustainable future aviation. The double wing system of the PrP, including the side wings connectors, allows the installation of multiple control effectors. This poses an interesting design challenge, as shown in [12, 13], and at the same time enables original and innovative control possibilities, like Direct Lift Control (DLC) and Direct Side-Force Control. The aircraft configuration is shown in Fig. 2.

The aircraft geometry is created in the Multi Model Generator (MMG), an in-house developed Knowledge Based Engineering (KBE) toolbox [14]. This tool provides automatic, configuration-agnostic modeling and meshing capabilities, which can be interfaced with selected aerodynamic solvers. By making use of the commercial panel method code VSAERO [15], a vast aerodynamic database for the PrP has been generated in the form of look-up tables. The database for steady aerodynamics expresses the six non-dimensional aerodynamic actions in Body Axes

$$\left\{C_{X_\mathrm{B}}, C_{Y_\mathrm{B}}, C_{Z_\mathrm{B}}, C_{\mathcal{L}_\mathrm{B}}, C_{\mathcal{M}_\mathrm{B}}, C_{\mathcal{N}_\mathrm{B}}\right\}^{\mathcal{A}} \tag{8}$$

as tabular functions of α, β, M_∞ and control surface deflections $\boldsymbol{\delta}$. Dynamic derivatives with respect to rotational rates p, q, r are calculated for each flight condition with a second order finite difference formula. Each of the six aerodynamic actions in Eq. 8 is then expressed as the following superposition of effects:

$$C_F^{\mathcal{A}} = \underbrace{C_{F_0}(\alpha, \beta, M_\infty, \boldsymbol{\delta} = \mathbf{0})}_{\text{steady, clean}} + \underbrace{\sum_{i=1}^{N_\delta} \Delta C_F(\alpha, \beta, M_\infty, \delta_i)}_{\text{steady, control effectors}} + \underbrace{\sum_{\omega=p,q,r} C_{F_\omega}(\alpha, \beta, M_\infty, \boldsymbol{\delta} = \mathbf{0})\,\omega}_{\text{unsteady, clean}}. \tag{9}$$

For the aerodynamic database used in the present study, both α and β range from $-6°$ to $6°$ in steps of $3°$, while two mach numbers have been analyzed, namely $M_\infty = 0.3$ and $M_\infty = 0.6$. Additionally, each control surface has been deflected, independently from all the others, from $-30°$ to $30°$ in steps of $10°$.

The aerodynamic database is imported in the Performance, Handling Qualities, and Loads Analysis Toolbox (PHALANX). This is a non-linear simulation and analysis toolbox, which integrates data and sub-models from various aeronautical disciplines (aerodynamics, propulsion, flight control system, weight and balance, etc.), in order to generate a complete Flight Mechanics Model (FMM) of the aircraft. PHALANX is developed in MATLAB®/Simulink and revolves around a Simscape Multibody Dynamics core. This allows to model and simulate systems dynamics without the need to explicitly write the analytical equations of motion. In this way, it is possible to model complex phenomena like relative motion of aircraft parts (e.g. center of gravity due to fuel consumption) or wing flexibility, and measure local flight parameters at specific aircraft locations. For the current work, with the aircraft having neither moving parts, nor variable mass components and not interacting with the ground, the underlying equations of motion reduce to the

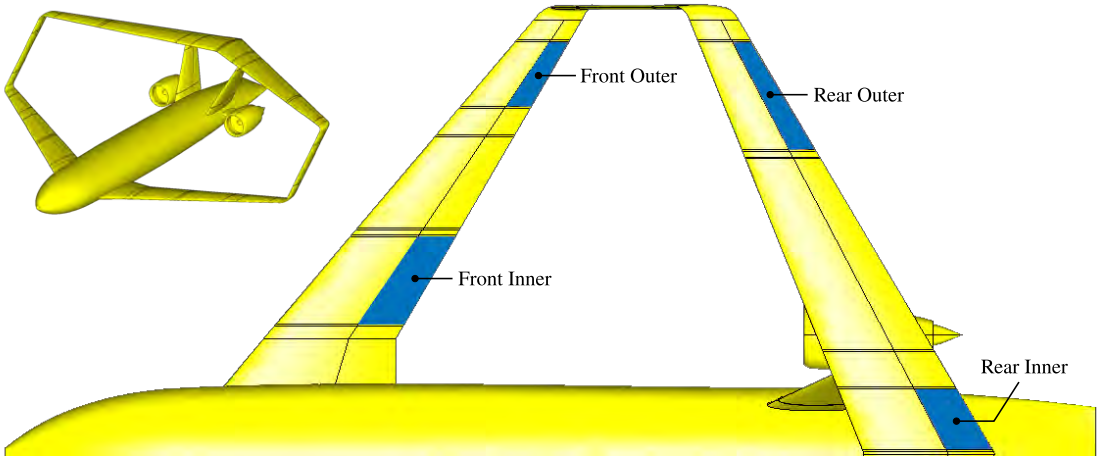

Fig. 2 PrP aircraft configuration as modeled in the MMG, with control surfaces highlighted on the main wings.

classic 6-DoF rigid body dynamic equations, written in Body Axes:

$$\begin{aligned}
\begin{Bmatrix} \dot{u} \\ \dot{v} \\ \dot{w} \end{Bmatrix} &= -\begin{Bmatrix} p \\ q \\ r \end{Bmatrix} \times \begin{Bmatrix} u \\ v \\ w \end{Bmatrix} + \frac{g}{W} \begin{Bmatrix} C_{X_\mathrm{B}}(\alpha,\beta,\theta,\phi,\boldsymbol{\delta}) - W\sin\theta \\ C_{Y_\mathrm{B}}(\alpha,\beta,\theta,\phi,\boldsymbol{\delta}) + W\sin\phi\cos\theta \\ C_{Z_\mathrm{B}}(\alpha,\beta,\theta,\phi,\boldsymbol{\delta}) + W\cos\phi\cos\theta \end{Bmatrix} \\
\begin{Bmatrix} \dot{p} \\ \dot{q} \\ \dot{r} \end{Bmatrix} &= I^{-1}\left(-\begin{Bmatrix} p \\ q \\ r \end{Bmatrix} \times I \begin{Bmatrix} p \\ q \\ r \end{Bmatrix} + \begin{Bmatrix} C_{\mathcal{L}_\mathrm{B}}(\alpha,\beta,\theta,\phi,\boldsymbol{\delta}) \\ C_{\mathcal{M}_\mathrm{B}}(\alpha,\beta,\theta,\phi,\boldsymbol{\delta}) \\ C_{\mathcal{N}_\mathrm{B}}(\alpha,\beta,\theta,\phi,\boldsymbol{\delta}) \end{Bmatrix} \right)
\end{aligned} \tag{10}$$

The toolbox is aircraft configuration-agnostic and data-driven, meaning that its fidelity depends on the data and formulations used in the sub-models. This allows PHALANX to operate consistently at different stages of the aircraft design process. The toolbox has been used in the past for the positioning and sizing of control surfaces of the PrP [12, 13], and the analysis and simulation of novel aircraft configurations like the BWB [16] and the Delft University Unconventional Configuration (DUUC), featuring the propulsive empennage concept [17].

III. Theoretical background

As mentioned previously, control authority is here defined as the ability of the control effectors to generate forces and moments (or *generalized forces*) in the selected direction of one or more motion axes of interest. It is here indicated with the symbol $\mathcal{A}_{\pm F}$. For example, pitch-up control authority is defined as the ability to generate the largest pitch-up moment, i.e. the largest positive moment about the pitch axis, from a given reference condition. It is calculated as

$$\mathcal{A}_{+\mathcal{M}} = \left| C_{\mathcal{M}}^{\max} - C_{\mathcal{M}}^{\mathrm{ref}} \right|. \tag{11}$$

In a similar fashion, pitch-down control authority is defined as the ability to generate the largest negative moment about the pitch axis, and is calculated as

$$\mathcal{A}_{-\mathcal{M}} = \left| C_{\mathcal{M}}^{\min} - C_{\mathcal{M}}^{\mathrm{ref}} \right|. \tag{12}$$

Because $C_{\mathcal{M}}^{\max}$ and $C_{\mathcal{M}}^{\min}$ are, in general, quantities of opposite sign, the control authorities $\mathcal{A}_{+\mathcal{M}}$ and $\mathcal{A}_{-\mathcal{M}}$ are very different in magnitude, for the same reference condition. When more than one motion axis is of interest, the definition can be extended to the norm of a vector quantity:

$$\mathcal{A}_{\boldsymbol{F}} = \left\| C_{\boldsymbol{F}}^{\mathrm{lim}} - C_{\boldsymbol{F}}^{\mathrm{ref}} \right\|. \tag{13}$$

Although control authority is a function of all flight and aircraft configuration parameters, for a given flight condition $\{\alpha, \beta, M_\infty\}$ it only depends on the position of the control effectors. In this case, it can be expressed in terms of the aerodynamic actions due to the control effectors $\Delta C_{\boldsymbol{F}}$:

$$\Delta\mathcal{A}_{\boldsymbol{F}} = \left\| \Delta C_{\boldsymbol{F}}^{\mathrm{lim}} - \Delta C_{\boldsymbol{F}}^{\mathrm{ref}} \right\|. \tag{14}$$

This definitions are used in the following subsections, where more concepts related to CA theory are recalled.

A. The Attainable Moment Set

In order to visualize the definition given in Eq. 14, and understand its geometrical interpretation, it is useful to recall the definitions of *Control Space* and *Moment Space*, as defined in [6]:

- **Control Space** is a Cartesian axis system in the $\mathbb{R}^{N_\delta}$ space, with a control effector position varying on each axis. Each combination of control effectors positions is represented by a point in Control Space. The set of all possible effectors positions is called the Admissible Controls Set (ACS). If the effectors positions are simply bounded, the ACS is a hyper-rectangle in Control Space (i.e. a rectangle in $\mathbb{R}^2$, a parallelepiped in $\mathbb{R}^3$, etc.).
- **Moment Space** is a Cartesian axis system in the $\mathbb{R}^{N_{\boldsymbol{F}}}$ space, with a generalized force varying on each axis. The generalized forces generated by a combination of effectors positions are represented by a point in Moment Space. The set of all possible generalized forces generated by the effectors is called the Greatest Attainable Moment Set (GAMS).

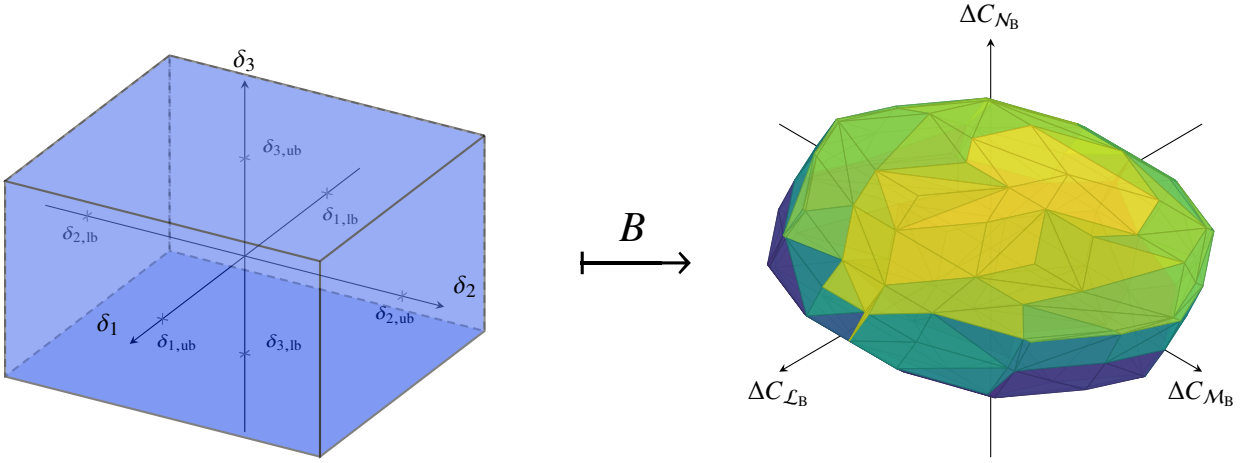

a) Generic Admissible Control Set in $\mathbb{R}^3$

b) Generic Greatest Attainable Moment Set in $\mathbb{R}^3$ for the classic "three moment" allocation

Fig. 3 Mapping of the Admissible Control Set (ACS) to the Greatest Attainable Moment Set (GAMS) through the control effectiveness matrix B. In this specific example, both the AMS and the GAMS are subspaces of $\mathbb{R}^3$.

It should be clear, at this point, how the GAMS is a function of the ACS. As shown in Eq. 9, for a given flight condition, the aerodynamic actions on the aircraft are related to the effectors position through the control-dependent part of the non-linear aerodynamic model. Due to non-linearities and couplings in the aerodynamic model, it is usually hard to characterize the GAMS in Moment Space. One notable analytic effort is presented in [18]. If Eq. 9 is linearized w.r.t. the control effectors positions, the control effectiveness matrix B is introduced:

$$B = \frac{\partial C_{\boldsymbol{F}}}{\partial \boldsymbol{\delta}} = \frac{\partial \Delta C_{\boldsymbol{F}}}{\partial \boldsymbol{\delta}} = \begin{bmatrix} \partial C_{F_1}/\partial \delta_1 & \partial C_{F_1}/\partial \delta_2 & \dots & \partial C_{F_1}/\partial \delta_{N_{\boldsymbol{\delta}}} \\ \partial C_{F_2}/\partial \delta_1 & \partial C_{F_2}/\partial \delta_2 & \dots & \partial C_{F_2}/\partial \delta_{N_{\boldsymbol{\delta}}} \\ \vdots & \vdots & \ddots & \vdots \\ \partial C_{F_{N_{\boldsymbol{F}}}}/\partial \delta_1 & \partial C_{F_{N_{\boldsymbol{F}}}}/\partial \delta_2 & \dots & \partial C_{F_{N_{\boldsymbol{F}}}}/\partial \delta_{N_{\boldsymbol{\delta}}} \end{bmatrix}. \tag{15}$$

If the aircraft has $N_{\boldsymbol{\delta}}$ control effectors and $N_{\boldsymbol{F}}$ controlled forces, B defines a linear function

$$\begin{aligned} B\colon \ \mathbb{R}^{N_{\boldsymbol{\delta}}} &\to \mathbb{R}^{N_{\boldsymbol{F}}} \\ \boldsymbol{\delta} &\mapsto \Delta C_{\boldsymbol{F}} = B\boldsymbol{\delta} \end{aligned} \tag{16}$$

which maps the ACS to an approximation of the GAMS. The goodness of such approximation depends on how accurately the linear model of Eq. 16 represents the non-linear one of Eq. 9 for the selected flight condition.

If B is constant and with the ACS being a convex set, it can be proven that the GAMS is a bounded convex polytope set in $\mathbb{R}^{N_{\boldsymbol{F}}}$ (i.e. a polygon in $\mathbb{R}^2$, a polyhedron in $\mathbb{R}^3$, etc.) [19], as shown in Fig. 3. The geometric algorithm to construct the GAMS, given a constant B matrix and the effectors positions saturation limits, is described in [6] for $N_{\boldsymbol{F}} = 2$ and $N_{\boldsymbol{F}} = 3$. In this work, it has been generalized to any number of generalized forces.

The convexity of the GAMS guarantees the existence of an interior and of a boundary of the GAMS. The generalized trim control forces $\Delta C_{\boldsymbol{F}}^{\mathrm{tr}}$ are represented by a point belonging to the interior or to the boundary of the GAMS corresponding to the given trim flight condition. The inverse is obviously not true: not all points belonging to the interior or the boundary of the GAMS are trim points. Within this scope, trimming the aircraft means finding the flight condition and the set of control aerodynamic actions $\Delta C_{\boldsymbol{F}}^{\mathrm{tr}}$, lying inside or on the boundary of the corresponding GAMS, so that Eq. 2 is verified.

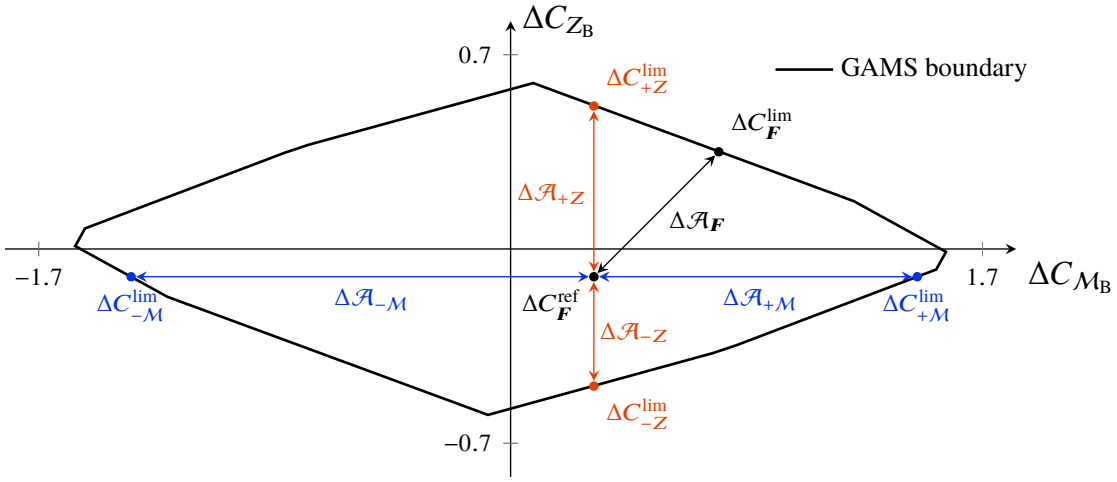

Fig. 4 Geometric interpretation of control authority about various motion axes and directions in an $\mathbb{R}^2$ Moment Space. The GAMS for the lift force and pitch moment allocation has been obtained for $\alpha = 0°$, $\beta = 0°$ and $M_\infty = 0.5$ at standard sea level conditions.

B. Control Authority

In light of the formal definitions given with Eq. 13 and Eq. 14, it is clear that control authority is not expressed in terms of effectors positions, but in terms of the actual generalized forces. It is therefore a quantity which lives in Moment Space, and in particular within the GAMS.

The reference combination of generalized control forces $\Delta C^{ref}_{\boldsymbol{F}}$ is represented by a point in the interior or on the boundary of the GAMS: this is going to be referred to as the *reference point*. The limit combination of attainable generalized control forces $\Delta C^{lim}_{\boldsymbol{F}}$ is represented by a point on the boundary of the GAMS: this is going to be referred to as the *limit point*. The limit point is found at the intersection of the GAMS boundary and a half-line having the initial point in $\Delta C^{ref}_{\boldsymbol{F}}$ and the prescribed control authority direction in Moment Space. With respect to a given direction in Moment Space, control authority is then represented as the distance between the reference point and the limit point, as shown in Fig. 4.

Trimming the aircraft for maximum control authority along a specific axis and direction (e.g. pitch-up) means finding $\Delta C^{ref}_{\boldsymbol{F}} = \Delta C^{tr}_{\boldsymbol{F}}$ in the interior or on the boundary of the GAMS, so that its distance from $\Delta C^{lim}_{\boldsymbol{F}}$ is maximum and Eq. 2 is verified. The trim problem formulation for maximum control authority is formalized in Sec. IV.

C. Control Allocation

Every point $\Delta C_{\boldsymbol{F}}$ in Moment Space has to be associated with a combination of control effectors positions $\boldsymbol{\delta}$. This task constitutes the CA problem and, in the scope of the linear formulation shown in Eq. 16, resolves in inverting the control effectiveness matrix B. If the matrix is square, i.e. the number of controlled axes $N_{\boldsymbol{F}}$ is equal to the number of control effectors $N_{\boldsymbol{\delta}}$, the solution is unique and immediately determined. This is generally the case for conventional aircraft configurations with ganged control surfaces. Aircraft featuring redundant and/or unganged control effectors usually result in a B matrix having more columns than rows, which therefore cannot be inverted. A function or algorithm $f_{CA}(B)$ has then to be found to perform the CA, as previously shown in Eq. 7.

A vast variety of CA methods has been developed in the past, for both linear and non-linear aerodynamic models. Most CA algorithms rise from the formulation of an optimization problem. Some methods are targeted to simply minimize the difference between the requested and the generated generalized forces

$$\min_{\boldsymbol{\delta}} \mathcal{J} = \|\Delta C_{\boldsymbol{F}} - B\boldsymbol{\delta}\|, \tag{17}$$

while other algorithms do so while optimizing a secondary parameter, like total effectors displacement, trim drag [7, 8], or structural loads [20]. A detailed survey of CA methods is presented in [21].

As systematically demonstrated in [6], not all CA methods are capable of returning admissible control positions for every generalized force in the interior or on the boundary of the GAMS. In other words, not all CA methods are capable of mapping the GAMS in its entirety back to the ACS. If only a subset of the GAMS, hence simply called Attainable

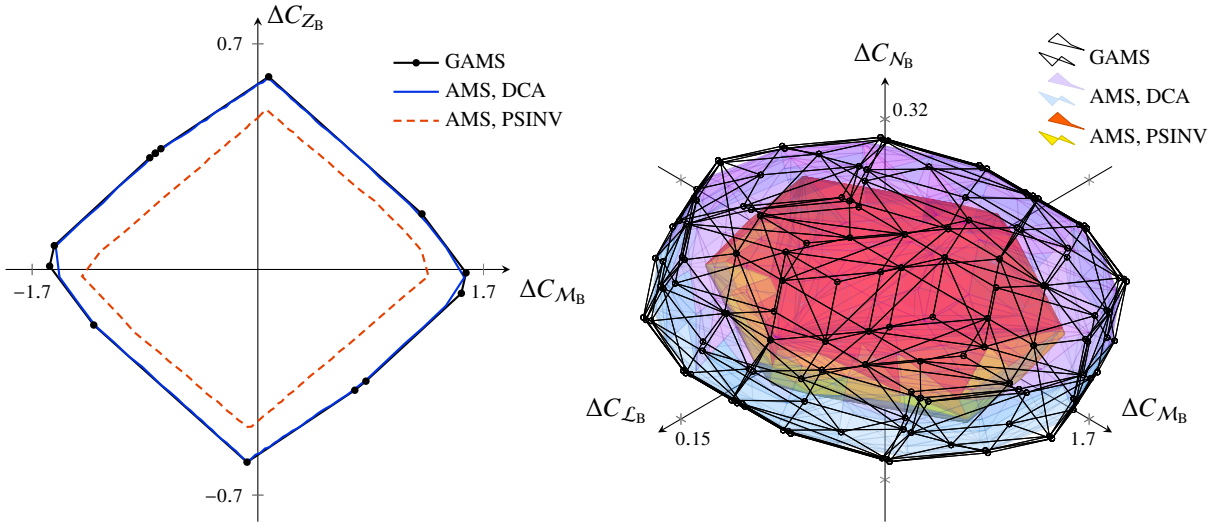

a) Lift force and pitch moment allocation

b) "Three moment" allocation

Fig. 5 Comparison of GAMS with AMS of different CA methods in $\mathbb{R}^2$ (*left*) and $\mathbb{R}^3$ (*right*), for $\alpha = 0°$, $\beta = 0°$ and $M_\infty = 0.5$ at standard sea level conditions. The DCA method is able to attain the complete GAMS, while the PSINV only a subset of it.

Moment Set (AMS), is achievable by the chosen CA algorithm, potentially attainable trim conditions would appear seemingly unattainable. This is of course undesired, as the calculation of trim conditions and of control authority would be limited by the CA method, and not by the physical possibilities allowed by the flight mechanics model.

In the current work, the Linear Programming (LP) formulation of the DCA method presented in [22] is used, for it yields several advantages over the original, geometry based formulation presented in [6]. Namely, the LP-DCA method converts the classic, direction-preserving DCA problem

$$\left.\begin{aligned} \max_{\boldsymbol{\delta}} \quad & \mathcal{J} = \rho \\ \text{subj. to} \quad & \rho \Delta C_{\boldsymbol{F}} - B\boldsymbol{\delta} = 0 \\ & \boldsymbol{\delta}_{\text{lb}} \leq \boldsymbol{\delta} \leq \boldsymbol{\delta}_{\text{ub}} \end{aligned}\right\} \quad \text{with} \quad \boldsymbol{\delta} \leftarrow \boldsymbol{\delta}/\rho \quad \text{if} \quad \rho > 1 \tag{18}$$

to the smallest equivalent LP problem. It is able to attain 100% of the generalized forces in the GAMS, and it can be scaled to any number of controlled axes $N_{\boldsymbol{F}}$, mixing forces and moments, without loss of computational efficiency. In Fig. 5, the AMS of the LP-DCA method is compared to the GAMS and to the AMS of the simple, analytic Pseudo-Inverse (PSINV) CA method.

IV. Method and implementation

The trim problem is here formulated in a generic format that allows easily changing the number and type of trim controls while allowing a fair comparison between the analyses. The parameters that must be explicitly supplied for the trim problem to be initialized are the aircraft position in Earth Axes $\{X_E, Y_E, Z_E\}^{\text{tr}}$, the ground track orientation w.r.t. to local north $\psi_{\text{GT}}^{\text{tr}}$, the airspeed V^{tr}, and the Euler angular rates $\{\dot{\psi}, \dot{\theta}, \dot{\phi}\}^{\text{tr}}$. Obviously, specifying the ground track orientation is actually meaningful only in geo-referenced applications. In this application, using an abstract flat Earth model, such parameter has no influence on the outcome of the trim problem.

A. Trim controls and bound constraints

The trim controls set $\boldsymbol{\mathcal{X}}$ is conceptually separated into three subsets:

- the pilot subset $\boldsymbol{\Pi}$, composed by the normalized stick commands $\{\delta_{\text{lat}}, \delta_{\text{lon}}, \delta_{\text{dir}}\}$, and the throttle lever δ_{T};
- the attitudes subset $\boldsymbol{\Theta}$, comprising the flight path angle γ, the Euler angles $\{\psi, \theta, \phi\}$, and the side-slip angle β;
- the actions subset $\Delta C_{\boldsymbol{F}}$, containing the generalized control forces that are going to be allocated to the effectors.

In summary:

$$\mathcal{X} = \{\mathbf{\Pi}, \mathbf{\Theta}, \Delta C_{\boldsymbol{F}}\} \qquad \text{with} \quad \begin{aligned} \mathbf{\Pi} &= \{\delta_{\text{lat}}, \delta_{\text{lon}}, \delta_{\text{dir}}, \delta_{\text{T}}\} \\ \mathbf{\Theta} &= \{\gamma, \psi, \theta, \phi, \beta\} \\ \Delta C_{\boldsymbol{F}} &= \{\Delta C_X, \Delta C_Y, \Delta C_Z, \Delta C_{\mathcal{L}}, \Delta C_{\mathcal{M}}, \Delta C_{\mathcal{N}}\}. \end{aligned} \tag{19}$$

The subsets $\{\delta_{\text{lat}}, \delta_{\text{lon}}, \delta_{\text{dir}}\} \subset \mathbf{\Pi}$ and $\Delta C_{\boldsymbol{F}}$ are redundant and therefore mutually exclusive, as they share the purpose of generating control forces and moments. As the current work focuses on a trim problem formulation based on $\Delta C_{\boldsymbol{F}}$, the effective pilot subset of interest reduces to

$$\mathbf{\Pi} = \{\delta_{\text{T}}\}. \tag{20}$$

The throttle lever is a normalized variable ranging from -1 to 1, where the minimum value supplies engine idle thrust and the maximum value corresponds to supplying the total available engine thrust at the current flight condition.

In the formal trim problem formulation presented in Sec. IV.E, the normalized pilot controls $\mathbf{\Pi}$ are bounded to the interval $[-1,\ 1]$, the attitude angles $\mathbf{\Theta}$ are bounded to the interval $[-\pi/2,\ \pi/2]$, while the other trim controls are left unbounded.

B. Equality constraints

A certain number of equality constraints has to be prescribed to assure that the trim problem is well-posed. This is generally requested to prevent the existence of explicit relations among trim controls that are state variables [1]. In the proposed implementation, if the equality constraint assigns a numeric value directly to a trim control, that trim control is considered as an explicitly initialized variable and the constraint is removed. In all of the presented application cases, the flight path and side-slip angles are constrained in either one of the following ways:

$$\gamma^{\text{tr}} = 0 \quad \text{and} \quad \beta^{\text{tr}} = 0 \tag{21a}$$

$$\gamma^{\text{tr}} = 0 \quad \text{and} \quad \beta^{\text{tr}} = V_{\text{SW}}/V^{\text{tr}}. \tag{21b}$$

Both are representative of horizontal flight conditions, respectively with no side-slip and with maximum side-slip required by regulations [23]. Since the ground track orientation ψ_{GT} is prescribed, Eq. 21b can be interpreted as a horizontal flight with forward slip. Constraining β is not strictly necessary for posing the trim problem correctly, but rather necessary to uniquely identify the desired flight condition. Forcing this extra initial value has to be complemented by an additional condition on β in either the objective function or the non-linear constraints of the optimization problem.

The resulting effective trim controls are here collected:

$$\mathcal{X} = \{\delta_{\text{T}}, \psi, \theta, \phi, \Delta C_{\boldsymbol{F}}\}. \tag{22}$$

The engine throttle δ_{T} is mainly devoted to trimming for the prescribed airspeed. Given a fixed flight path angle γ^{tr}, the nose attitude angle θ is mainly devoted to trimming for the necessary angle of attack. The remaining attitude angles are devoted to accomplishing the prescribed side-slip and lateral-directional forces. Finally, the control actions are devoted to the minor force adjustments, the equilibrium about the aircraft center of mass and, in the presented case, for achieving desired control authority.

As $\Delta C_{\boldsymbol{F}}$ contains from one to six variables, depending on which generalized forces are to be allocated, the trim controls set of Eq. 22 contains from five to ten variables, regardless of the aircraft configuration. An alternative formulation including control effectors positions would result in a minimum of seven trim controls, assuming the conventional three ganged control surfaces. For the presented PrP design, featuring twelve control surfaces including rudders on the twin vertical tails and drag-rudders on the side wings, it would result in sixteen trim controls.

C. Inequality constraints

A set of linear inequality constraints, together with additional equality constraints, is enforced for the generalized control forces $\Delta C_{\boldsymbol{F}}$, as shown in Eq. 23.

$$A^{ineq}_{\text{CH}}\, \Delta C_{\boldsymbol{F}} \leq b^{ineq}_{\text{CH}} \tag{23a}$$

$$A^{eq}_{\text{CH}}\, \Delta C_{\boldsymbol{F}} = b^{eq}_{\text{CH}} \tag{23b}$$

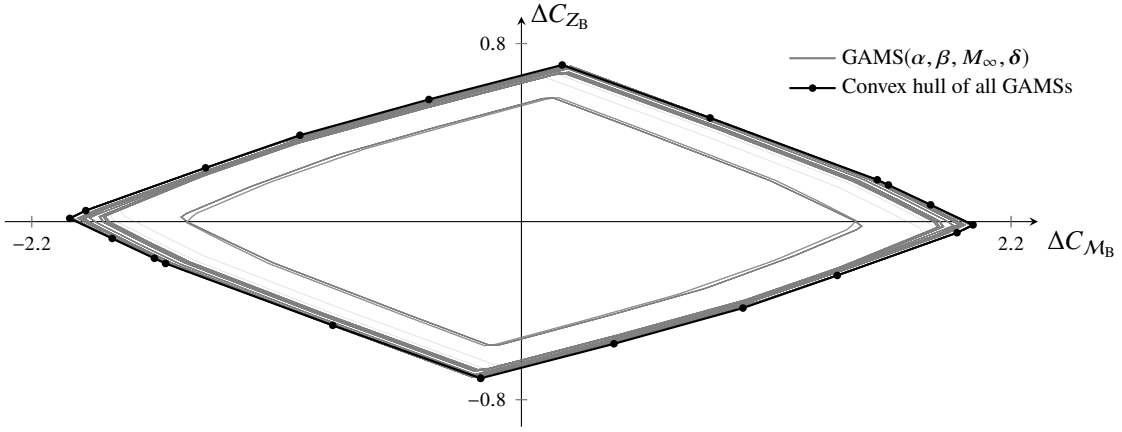

Fig. 6 Estimation of the convex hull of the most elongated GAMSs in $\mathbb{R}^2$. In this particular example, the convex hull corresponds to 16 inequality constraints for the generalized trim control forces.

These relations imply that each point $\Delta C_{\boldsymbol{F}}$ has to be in the interior or on the boundary of the GAMS. In particular, the A matrices and b column arrays constitute the Linear Constraint Representation (LCR) of the convex hull containing the most elongated GAMSs in all allocated directions:

$$\text{LCR}_{\text{CH}} = \left\{ A_{\text{CH}}^{ineq},\ b_{\text{CH}}^{ineq},\ A_{\text{CH}}^{eq},\ b_{\text{CH}}^{eq} \right\} \tag{24}$$

and have been calculated using the `vert2lcon` algorithm in MATLAB [24]. The inequalities in Eq. 23 are always well defined because the convex hull is, by definition, a convex set. The equalities are non-null if any of the edges, facets, or $(N_{\boldsymbol{F}} - 1)$-dimensional elements constituting the boundary of the convex hull is parallel to any reference axis in Moment Space. The most elongated GAMS in a given direction in Moment Space is found by varying flight parameters α, β and M_∞, and effectors positions $\boldsymbol{\delta}$ to obtain the control effectiveness matrix B which results in the GAMS spanning the most distance in that direction. Once the most elongated GAMS in every assigned direction is obtained, the convex hull of these can easily be calculated, as shown in Fig. 6. This is not a GAMS itself, but rather is the smallest convex set containing all the most elongated GAMSs. Hence serves a good purpose to establish the inequality constraints for the trim problem.

With this approach, the number of inequality constraints depends on the dimension of Moment Space $N_{\boldsymbol{F}}$, and on the number of control effectors $N_{\boldsymbol{\delta}}$. For large problems, it can go up to the order of magnitudes of thousand. An alternative approach to construct such constraints would consist in wrapping the convex hull of all GAMSs in its bounding hyper-rectangle, i.e. the smallest hyper-rectangle that contains the convex hull. In this case, the inequality constraints will only be $2N_{\boldsymbol{F}}$, corresponding to the $2N_{\boldsymbol{F}}$ boundary elements of the hyper-rectangle (e.g. 4 edges of a rectangle in $\mathbb{R}^2$, 6 faces of a parallelepiped in $\mathbb{R}^3$, etc.).

D. Objective function

Two objective functions are presented in the current work. In this section, it is shown how they are traced back to the common trim minimization problem formulation presented in the following Sec. IV.E. This is easily achieved as the calculation of both objective functions revolves around the same conceptual approach. Each objective function is calculated through an optimization sub-problem, revolving around the calculation of a certain limit point in Moment Space. The objective functions and their respective limit points are characterized in the following sub-sections.

1. Sub-Problem 1

It consists in maximizing control authority in a specified direction in Moment Space, $\mathcal{A}_{\pm F}$. Given such direction, the limit point is found at the intersection of the GAMS with a half-line ℓ having the specified direction and the initial point in $\Delta C_{\boldsymbol{F}}^{\text{ref}}$, as already shown in Fig. 4. The limit point is then characterized by the following condition: it is the furthest point from $\Delta C_{\boldsymbol{F}}^{\text{ref}}$ which simultaneously belongs to the half-line ℓ and the GAMS. In order to calculate it, the half-line ℓ is constructed geometrically and expressed in terms of its own LCR. The following optimization sub-problem results in

the limit point $\Delta C_{\boldsymbol{F}}^{\lim}$ and its distance w.r.t. the reference point $\Delta C_{\boldsymbol{F}}^{\text{ref}}$:

$$\Delta C_{\boldsymbol{F}}^{\lim} = \arg\left\{\begin{array}{ll}\max\limits_{\Delta C_{\boldsymbol{F}}} & \mathcal{J}^{\lim} = \left\|\Delta C_{\boldsymbol{F}} - \Delta C_{\boldsymbol{F}}^{\text{ref}}\right\| \\ \\ \text{subj. to} & \Delta C_{\boldsymbol{F}} \in \{\text{GAMS} \cap \ell\}\end{array}\right\} = \arg\left\{\begin{array}{ll}\max\limits_{\Delta C_{\boldsymbol{F}}} & \mathcal{J}^{\lim} = \left\|\Delta C_{\boldsymbol{F}} - \Delta C_{\boldsymbol{F}}^{\text{ref}}\right\| \\ \\ \text{subj. to} & A_{\text{CH}}^{ineq}\ \Delta C_{\boldsymbol{F}} \leq b_{\text{CH}}^{ineq} \\ & A_{\text{CH}}^{eq}\ \Delta C_{\boldsymbol{F}} \leq b_{\text{CH}}^{eq} \\ & A_{\ell}^{ineq}\ \Delta C_{\boldsymbol{F}} \leq b_{\ell}^{ineq} \\ & A_{\ell}^{eq}\ \Delta C_{\boldsymbol{F}} \leq b_{\ell}^{eq}\end{array}\right\} \tag{25}$$

$$\mathcal{J}_*^{\lim} = \mathcal{J}_{|\Delta C_{\boldsymbol{F}}^{\lim}}^{\lim} = \left\|\Delta C_{\boldsymbol{F}}^{\lim} - \Delta C_{\boldsymbol{F}}^{\text{ref}}\right\| = \mathcal{A}_{\pm F} \tag{26}$$

Because the purpose of Sub-Problem 1 is to *maximize* $\mathcal{A}_{\pm F}$ as a function of $\Delta C_{\boldsymbol{F}}^{\text{ref}}$, the objective function to be *minimized* in the actual trim optimization problem is

$$\mathcal{J}^{\text{tr}} = -\mathcal{J}_*^{\lim}\left(\Delta C_{\boldsymbol{F}}^{\text{ref}}\right) = -\left\|\Delta C_{\boldsymbol{F}}^{\lim} - \Delta C_{\boldsymbol{F}}\right\| = -\mathcal{A}_{\pm F}. \tag{27}$$

2. Sub-Problem 2

It consists in maximizing a balanced control authority in all directions in Moment Space, $\overline{\mathcal{A}}$. The maximum balanced control authority is here conveniently defined through the characterization of its corresponding limit point $\Delta C_{\boldsymbol{F}}^{\lim}$. The limit point with maximum $\overline{\mathcal{A}}$ is the point in the interior of the GAMS which has the maximum sum and the minimum variance of its distances to the GAMS vertices. Hence the chosen nomenclature: *maximum balanced* control authority. Such limit point corresponds to the centroid of the GAMS and, in case all the control effectors saturation limits are symmetric, with the origin of Moment Space. It is calculated with the following optimization sub-problem:

$$\Delta C_{\boldsymbol{F}}^{\lim} = \arg\left\{\begin{array}{ll}\max\limits_{\Delta C_{\boldsymbol{F}}} & \mathcal{J}^{\lim} = \dfrac{\sum_{i=1}^{n} d_i}{\frac{1}{n}\sum_{i=1}^{n}\left|d_i - \frac{\sum_{i=1}^{n} d_i}{n}\right|^2} \\ \\ \text{subj. to} & \Delta C_{\boldsymbol{F}} \in \text{GAMS}\end{array}\right\} = \arg\left\{\begin{array}{ll}\max\limits_{\Delta C_{\boldsymbol{F}}} & \mathcal{J}^{\lim} = \dfrac{\sum_{i=1}^{n} d_i}{\frac{1}{n}\sum_{i=1}^{n}\left|d_i - \frac{\sum_{i=1}^{n} d_i}{n}\right|^2} \\ \\ \text{subj. to} & A_{\text{CH}}^{ineq}\ \Delta C_{\boldsymbol{F}} \leq b_{\text{CH}}^{ineq} \\ & A_{\text{CH}}^{eq}\ \Delta C_{\boldsymbol{F}} \leq b_{\text{CH}}^{eq}\end{array}\right\} \tag{28}$$

where d_i is the distance between the candidate point $\Delta C_{\boldsymbol{F}}$ and the i-th vertex of the GAMS, and n is the number of vertices of the GAMS. Once the limit point has been found, the actual trim problem to maximize $\overline{\mathcal{A}}$ can be formulated in terms of *minimizing* the distance from the candidate trim point to the just found limit point. In other words, the objective function to be *minimized* in the actual trim optimization problem, for Sub-Problem 2, is

$$\mathcal{J}^{\text{tr}} = \left\|\Delta C_{\boldsymbol{F}}^{\lim} - \Delta C_{\boldsymbol{F}}\right\|. \tag{29}$$

E. Trim problem formulation

In summary, the trim approach corresponding to Sub-Problem 1 will *maximize* the distance from the trim point to the limit point which lies on the boundary of the GAMS in the given direction in Moment Space. The trim approach corresponding to Sub-Problem 2 will *minimize* the distance from the trim point to the centroid of the GAMS.

With the objective function being defined by either Eq. 27 or Eq. 29, and the bounds and constraints introduced in the previous sections, the trim problem can now be formulated in the following general format:

$$\begin{array}{ll}\min\limits_{\mathcal{X}=\{\boldsymbol{\Pi},\boldsymbol{\Theta},\Delta C_{\boldsymbol{F}}\}} & \mathcal{J}^{\text{tr}} = \mathcal{J}^{\text{tr}}(\mathcal{X}) \\ \\ \text{subj. to} & \boldsymbol{-1} \leq \boldsymbol{\Pi} \leq \boldsymbol{1} \\ & \boldsymbol{-\pi/2} \leq \boldsymbol{\Theta} \leq \boldsymbol{\pi/2} \\ & \boldsymbol{f}(\mathcal{X}_0, \mathcal{X}) = \boldsymbol{0} \\ & A_{\text{CH}}^{ineq}\ \Delta C_{\boldsymbol{F}} \leq b_{\text{CH}}^{ineq} \\ & A_{\text{CH}}^{eq}\ \Delta C_{\boldsymbol{F}} \leq b_{\text{CH}}^{eq}\end{array} \tag{30}$$

The problem is solved with the `fmincon` routine in MATLAB®, using the interior-point algorithm. Because the problem is non-smooth, due to the sharp corners in the geometry of the GAMS, the termination criterion for the solver is based on the step size and on the variation of the objective function. Constraints are respected with a tolerance of 10^{-6}.

Due to the iterative nature of the algorithm, the solver finds local optima that, in general, depend on the first-guess values of the trim controls. At each iteration, the control effectiveness matrix B is calculated using the current value of α, β, M_∞, and the value of $\boldsymbol{\delta}$ from the previous trim iteration. Hence the GAMS geometry and the evaluation of control authority evolve throughout the optimization, and are not frozen to the moment of the problem initialization. The effectors positions $\boldsymbol{\delta}$ are calculated as exaplained in Sec. III.C.

F. Examples

Three examples with Moment Space in $\mathbb{R}^2$ are presented in Fig. 7, to visualize how the trim method operates. The cases cover a trim for maximum lift-up, maximum pitch-up and maximum balanced control authority. The control effectiveness matrix is calculated in Aerodynamic Axes, so that lift L is the force component lying in the negative direction of the Z_A axis.

In the figure, it is noticeable how the three optimal trim points are lying approximately on the same horizontal coordinate, i.e. in all three cases the effectors generate approximately the same control pitch moment necessary for rotational equilibrium about the aircraft center of gravity. On the other hand, the control-dependent lift changes quite significantly, together with the the angle of attack. This is explained by the possibility of the PrP wing to control lift and pitch moment *directly* in two different ways: by altering the angle of attack α, or by deflecting the front and rear control surfaces. The trim method capitalizes on this characteristic by distributing the required lift to α and $\boldsymbol{\delta}$ in order to optimize the assigned control authority.

V. Application and results

In a similar way as just done in the last section, the PrP model is trimmed in a prescribed flight condition while maximizing control authority in different directions. For this application, the fully non-linear, 6-DoF flight mechanics model is used. The set of allocated generalized forces is

$$\left\{C_L, C_{\mathcal{L}_\mathrm{A}}, C_{\mathcal{M}_\mathrm{A}}, C_{\mathcal{N}_\mathrm{A}}\right\} \tag{31}$$

in Aerodynamic Axes. This set constitutes the extension of the classic "three moment" CA problem, and it has been chosen for it yields improved results with respect to it, as shown in previous studies [5]. Being the GAMS a subset of $\mathbb{R}^4$, results cannot be shown in Moment Space for this application. Attention is focused on the resulting control surfaces deflections at trim, as well as on the remaining trim controls.

Trim is performed at standard sea level conditions for a horizontal trajectory, $\gamma^\mathrm{tr} = 0$, and an airspeed of $V^\mathrm{tr} = 170\,\mathrm{m\cdot s^{-1}}$, corresponding to $M_\infty = 0.5$. These conditions have been chosen to allow for sufficient control power about all axes, in order not to contaminate the proposed method with any model-induced limitation. In one case, no side-wind component is prescribed for the trim, and hence the aircraft is requested to fly straight and leveled. In the other case, the aircraft is required to trim in forward-slip condition by prescribing the maximum side-slip angle required by regulations for the given airspeed [23].

All of the twelve control surfaces available on the two main wings, the two side-wings and the two vertical tails are used to trim the aircraft. At every optimizer iteration, all control surfaces are initially commanded by the CA method shown in Sec. III.C. After the CA algorithm has converged, the deflection angles of the two rudders are averaged, and such average is re-assigned to both of them. The same is done for the movables on the two vertical side-wings. This partial ganging strategy has been necessary to prevent the appearance of opposite deflections, which would have resulted in using such control surfaces as drag rudders.

Results are compared for maximum control authority in both directions of the lift and pitch axes (lift-up, lift-down, pitch-up and pitch-down), and for maximum balanced control authority. Each trim problem, resulting from a given combination of objective function and assigned input parameters, has been simulated multiple times, with randomly generated initial values for the trim controls, until it converged successfully for five times. The convergence ratio is about 83% for the problems with $\beta = 0°$, with only one failed case before five were completed, while close to 50% for the problems with $\beta = 4.3°$. The resulting control surface deflections and flight parameters show, in general, little variability among different local optimal solutions of the same problem. A couple of extreme cases have been found, which exploit extrapolation of the aerodynamic database ($\alpha = -6.1°$) or unrealistic thrust levels ($\delta_\mathrm{T} = -1$) to find optimal trim

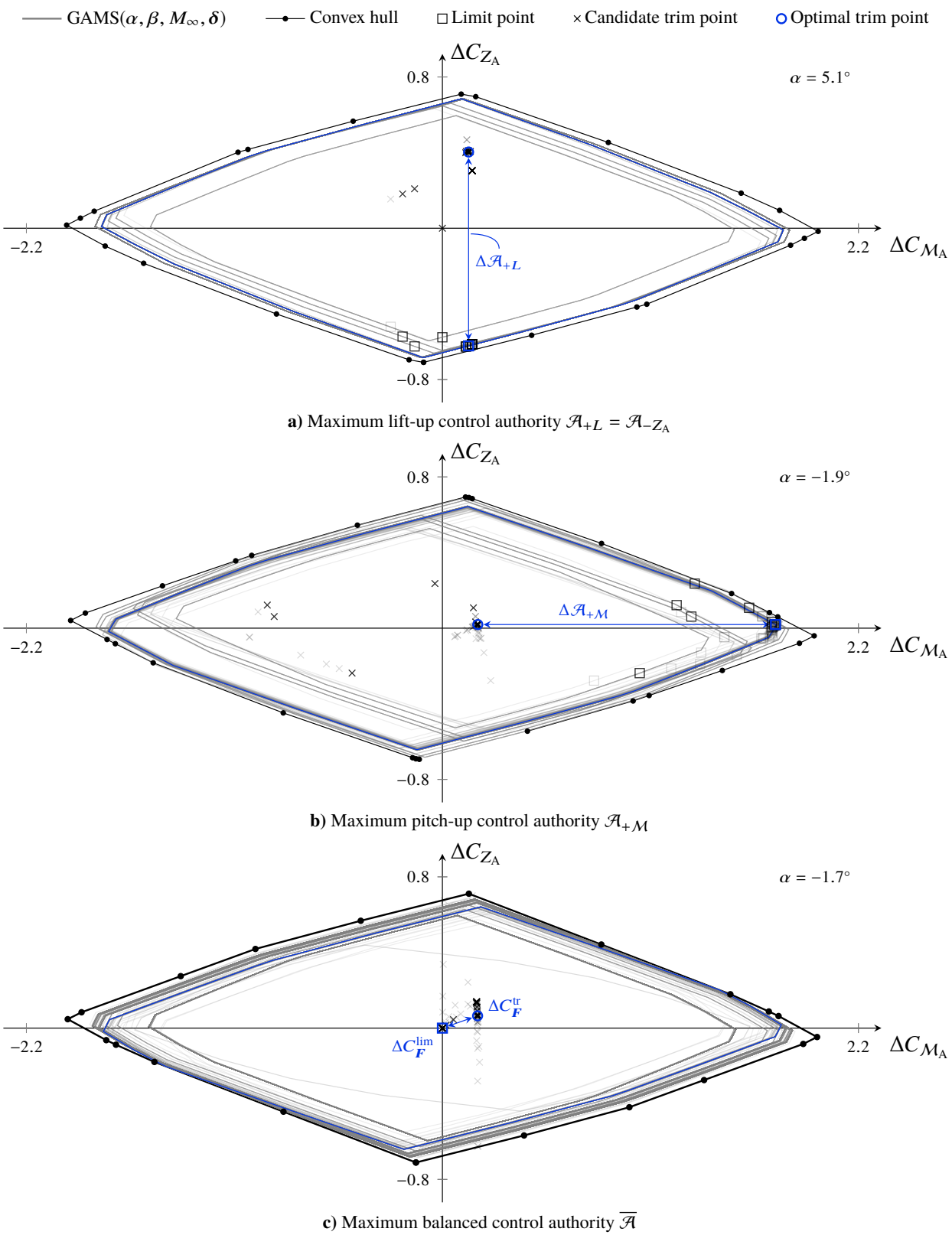

a) Maximum lift-up control authority $\mathcal{A}_{+L} = \mathcal{A}_{-Z_A}$

b) Maximum pitch-up control authority $\mathcal{A}_{+M}$

c) Maximum balanced control authority $\overline{\mathcal{A}}$

Fig. 7 Visualization in Moment Space of the trim optimization method presented in Sec. IV. Imposed trim conditions at sea level altitude: $V^{tr} = 170\,m{\cdot}s^{-1}$, $\gamma^{tr} = 0$. Non-linear, 3-DoF longitudinal-symmetric flight simulations.

conditions with better values of the objective function. This behavior could be easily removed by implementing stricter case-specific bounds and constraints in the optimization problem formulation. The extreme results have been filtered out, and the trim condition with the minimum value of the objective function is reported in Fig. 8. Control surface deflections on the main wings are positive if with trailing edge down, negative if with trailing edge up. The y-axis in the figure has been inverted to reflect this convention. The rudders deflections are positive if they cause the aircraft nose to point left of the flight path.

The symmetric flight condition allows to make the most interesting observations, as control surface deflections on the front wing range from the positive to the negative saturation limit, depending on which control authority is maximized. Maximum lift-up control authority is achieved with very negative deflections, both on the front and on the rear wing, paired up with a significant positive angle of attack $\alpha = 5.1°$. Maximum lift-down control authority is achieved with mostly large positive deflections at a negative angle of attack of $\alpha = -4.5°$. In both cases, it is evident how the control deflections are chosen to maximize control authority in the given direction, while the angle of attack is adjusted to guarantee vertical equilibrium. The maximum pitch-down control authority is achieved by exploiting the pitch-down moment due to the propulsion system. The throttle level is much higher in this case: this requires drastic positive deflections on the front wing and negative deflections on the rear wing to achieve equilibrium about the aircraft center of gravity. This is not observed in the case of control authority in the lift axis, as the slightly higher throttle setting is there justified by the higher magnitude of the angle of attack. On the other hand, the trim conditions for maximum pitch-up control authority are overall very similar to the one for maximum balanced control authority: both cases are characterized by the same throttle setting, and by small deflections on both the front and the rear wing. This behavior indicates how optimizing control authority about the pitch axis is a stiffer problem than optimizing it about the lift axis. As just observed, pitch control moment can be manipulated more significantly than control lift through the alteration of thrust. This couples the rotational equilibrium with the objective function and the horizontal equilibrium.

For the asymmetric flight condition, all the curves appear to have a similar shape, slightly shifting or stretching according to which control authority is maximized. The front inner surfaces are adjusted asymmetrically to provide for the necessary roll moment, together with the two tail rudders correcting for the directional moment. The front outer surfaces and all the rear ones are then adjusted for optimizing control authority. Trends in the remaining flight parameters are overall less evident and the numerical values less extreme. This happens because more control power is required to achieve trim, leaving less available control authority to the objective function.

In all cases, side-wing rudders are never used, due to their very small control effectiveness. Additionally, control surfaces on the front wing show more complex combinations of deflections than the ones on the rear wing, which are deflected by the same angle in all cases apart from one. This is justified by the fact that front control surfaces have a smaller moment arm with respect to the center of gravity, hence they are able to modulate control lift while retaining a small impact on control pitch.

VI. Conclusions

A definition of aerodynamic control authority has been given that is entirely based on generalized forces, and independent of the aircraft configuration and/or number of control effectors. A general trim problem formulation has been presented, in the form of an optimization problem, to trim a given aircraft model while maximizing control authority about one or more motion axes. The geometry of the Attainable Moment Set is used both for defining the inequality constraints, at the optimization problem set-up time, and for calculating the objective function of the problem itself. A Linear Programming Direct Control Allocation method has been used to map the generalized forces in the Attainable Moment Set to the control effectors positions. With application to an innovative box-wing aircraft called PrandtlPlane, the method is used to compare trim conditions for maximum control authority in the pitch axis, in the lift axis, and for maximum balanced control authority about all motion axes.

Results show that the method is able to capitalize on the angle of attack or the throttle setting to obtain the control surfaces deflections which maximize control authority in the assigned direction.

Future efforts can be devoted to validating this method when strongly non-linear aerodynamics is involved. For example, optimizing control authority about the drag axis could lead to a reformulation of the classic minimum trim drag problem, as well as interesting applications for trim in steep descent conditions. Additionally, time domain simulations to study the effect of the selected control authority are recommended. Given a specific maneuver to be performed after trim is achieved, a criterion to find which control authority has to be optimized to obtain best maneuver performance can be sought. Finally, the possibility to trim for specified lift-up/lift-down control force could effectively be used to specify the nose attitude angle at trim, which may be useful in certain scenarios like in-air refueling.

Name	Abbr.	Name	Abbr.	Name	Abbr.	Name	Abbr.
Front Left Outer	FLO	Left Side Wing	LSW	Rear Left Outer	RLO	Left Tail Rudder	LTR
Front Left Inner	FLI	Right Side Wing	RSW	Rear Left Inner	RLI	Right Tail Rudder	RTR
Front Right Inner	FRI			Rear Right Inner	RRI		
Front Right Outer	FRO			Rear Right Outer	RRO		

a) Control surfaces naming scheme

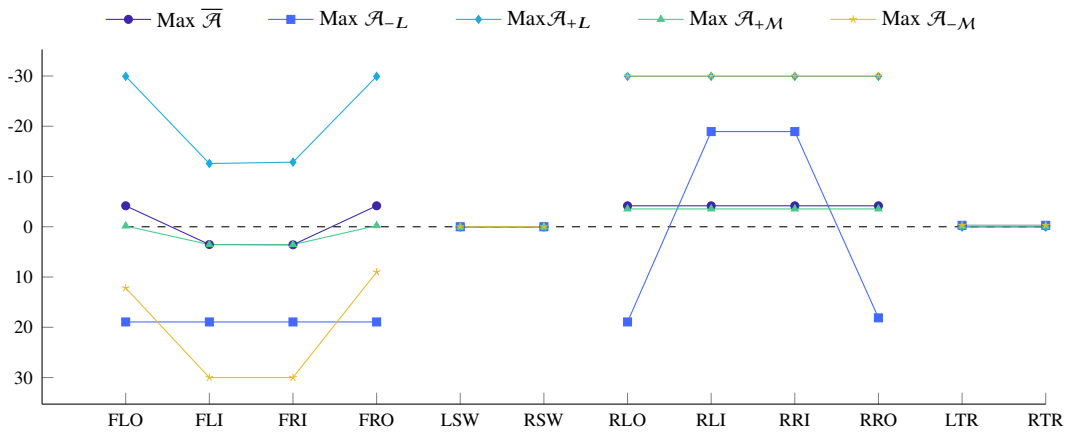

b) Control surface deflections in symmetric flight, with $\beta = 0°$. All trim conditions have wings leveled.

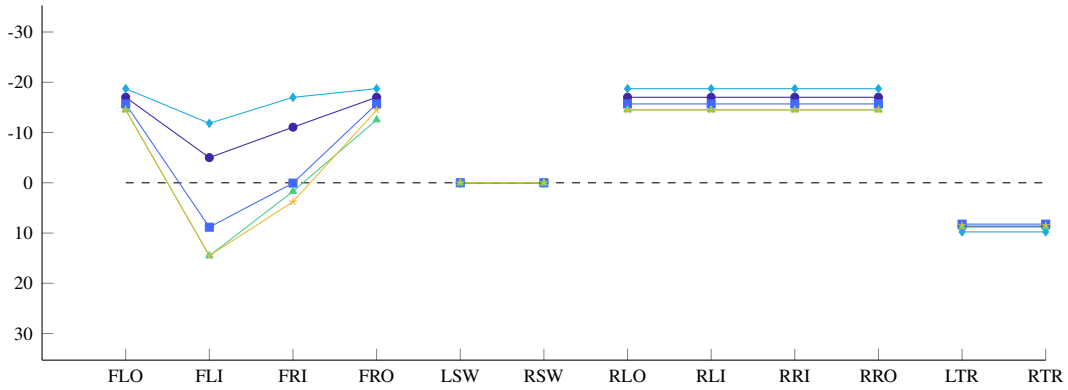

c) Control surface deflections in asymmetric flight, with $\beta = 4.3°$ forward-slip. All trim conditions are banked right with body heading slightly left of the ground track.

	$\beta^{\mathrm{tr}} = 0°$				$\beta^{\mathrm{tr}} = 4.3°$			
	$\alpha^{\mathrm{tr}} = \theta^{\mathrm{tr}}$	ϕ^{tr}	ψ^{tr}	$\delta_{\mathrm{T}}^{\mathrm{tr}}$	$\alpha^{\mathrm{tr}} = \theta^{\mathrm{tr}}$	ϕ^{tr}	ψ^{tr}	$\delta_{\mathrm{T}}^{\mathrm{tr}}$
Max $\overline{\mathcal{A}}$	−1.7°	0.1°	0.0°	0.18	2.9°	16.7°	−3.6°	0.40
Max $\mathcal{A}_{-L}$	−4.5°	0.2°	0.0°	0.56	1.4°	17.9°	−4.1°	0.53
Max $\mathcal{A}_{+L}$	5.1°	0.0°	0.0°	0.43	4.1°	16.2°	−3.3°	0.38
Max $\mathcal{A}_{+\mathcal{M}}$	−1.9°	0.1°	0.0°	0.19	0.9°	19.4°	−4.2°	−0.02
Max $\mathcal{A}_{-\mathcal{M}}$	−0.9°	−0.5°	0.0°	0.78	0.9°	18.8°	−4.2°	−0.05

d) Summary of other flight parameter

Fig. 8 Control surfaces deflections and other trim controls for symmetric and asymmetric trimmed flight, maximizing control authority about the pitch axis, the lift axis, and the balanced control authority. Imposed trim conditions at sea level altitude: $V^{\mathrm{tr}} = 170\,\mathrm{m\cdot s^{-1}}$, $\gamma^{\mathrm{tr}} = 0$. Non-linear, 6-DoF flight simulations.

Acknowledgments

The research presented in this paper has been carried out in the framework of the PARSIFAL (Prandtlplane ARchitecture for the Sustainable Improvement of Future AirpLanes) research project, which has been funded by the European Union within the Horizon 2020 Research and Innovation Program (Grant Agreement n.723149).

References

[1] Stevens, B. L., Lewis, F. L., and Johnson, E. N., *Aircraft Control and Simulation*, John Wiley & Sons, Ltd, 2016.

[2] Phillips, W. F., Hailey, C. E., and Gebert, G. A., "Review of Attitude Representations Used for Aircraft Kinematics," *Journal of Aircraft*, Vol. 38, No. 4, 2001, pp. 718–737. doi:10.2514/2.2824, URL https://doi.org/10.2514/2.2824.

[3] De Marco, A., Duke, E., and Berndt, J., "A General Solution to the Aircraft Trim Problem," *AIAA Modeling and Simulation Technologies Conference and Exhibit*, 2007. doi:10.2514/6.2007-6703, URL https://arc.aiaa.org/doi/abs/10.2514/6.2007-6703.

[4] Goodrich, K., Sliwa, S., and Lallman, F., "A Closed-Form Trim Solution Yielding Minimum Trim Drag for Airplanes with Multiple Longitudinal-Control Effectors," NASA Technical Paper 2907, National Aeronautics and Space Administration, 1989.

[5] Garmendia, D. C., and Mavris, D. N., "Alternative Trim Analysis Formulations for Vehicles with Redundant Multi-Axis Control Surfaces," *Journal of Aircraft*, Vol. 53, No. 1, 2016, pp. 60–72. doi:10.2514/1.C033184, URL https://doi.org/10.2514/1.C033184.

[6] Durham, W., Bordignon, K., and Beck, R., *Aircraft Control Allocation*, John Wiley & Sons, Ltd, 2017.

[7] Durham, W. C., Bolling, J. G., and Bordignon, K. A., "Minimum Drag Control Allocation," *Journal of Guidance, Control, and Dynamics*, Vol. 20, No. 1, 1997, pp. 190–193. doi:10.2514/2.4018, URL https://doi.org/10.2514/2.4018.

[8] Stolk, A., "Minimum drag control allocation for the Innovative Control Effector aircraft," Master's thesis, TU Delft, 2017.

[9] Cipolla, V., Abu Salem, K., Picchi Scardaoni, M., Frediani, A., and Binante, V., "Preliminary design and performance analysis of a box-wing transport aircraft," *AIAA SciTech Forum*, Orlando, Florida, USA, 2020.

[10] Carini, M., Meheut, M., and Kanellopoulos, S., "Aerodynamic analysis and optimization of a boxwing architecture for commercial airplanes," *AIAA SciTech Forum*, Orlando, Florida, USA, 2020.

[11] Prandtl, L., "Induced Drag of Multiplanes," NACA Technical Note 182, National Advisory Committee for Aeronautics, 1924.

[12] van Ginneken, D. A. J., Voskuijl, M., van Tooren, M. J. L., and Frediani, A., "Automated Control Surface Design and Sizing for the Prandtl Plane," *6th AIAA Multidisciplinary Design Optimization Specialist Conference*, 2010.

[13] Varriale, C., Raju Kulkarni, A., La Rocca, G., and Voskuijl, M., "A Hybryd, Configuration-Agnostic Approach to Aircraft Control Surface Sizing," *25th International Congress of the Italian Association of Aeronautics and Astronautics (AIDAA)*, 2019.

[14] Raju Kulkarni, A., Varriale, C., Voskuijl, M., La Rocca, G., and Veldhuis, L. L. M., "Assessment of Sub-scale Designs for Scaled Flight Testing," *AIAA Aviation Forum and Exposition*, American Institute of Aeronautics and Astronautics, 2019.

[15] Nathman, J. K., *VSAERO 7.9: A Computer Program for Calculating the Nonlinear Aerodynamic Characteristics of Arbitrary Configurations*, Stark Aerospace, Inc., 8440 154 th Avenue NE, Redmond, Washington 98052, USA, 2016.

[16] Voskuijl, M., La Rocca, G., and Dircken, F., "Controllability of Blended Wing Body Aircraft," *26th Congress of International Council of the Aeronautical Sciences*, 2008.

[17] Varriale, C., Hameeteman, K., Voskuijl, M., and Veldhuis, L., "A Thrust-Elevator Interaction Criterion for Aircraft Optimal Longitudinal Control," *AIAA Aviation Forum and Exposition*, Dallas, Texas, USA, 2019.

[18] Bolender, M. A., and Doman, D. B., "Method for Determination of Nonlinear Attainable Moment Sets," *Journal of Guidance, Control, and Dynamics*, Vol. 27, No. 5, 2004, pp. 907–914. doi:10.2514/1.9548, URL https://doi.org/10.2514/1.9548.

[19] Bordignon, K. A., "Constrained Control Allocation for Systems with Redundant Control Effectors," Ph.D. thesis, Virginia Polytechnic Institute and State University, 1996.

[20] Frost, S. A., Bodson, M., Burken, J. J., Jutte, C. V., Taylor, B. R., and Trinh, K. V., "Flight Control with Optimal Control Allocation Incorporating Structural Load Feedback," *Journal of Aerospace Information Systems*, Vol. 12, No. 12, 2015, pp. 825–834. doi:10.2514/1.I010278, URL https://doi.org/10.2514/1.I010278.

[21] Johansen, T. A., and Fossen, T. I., "Control allocation—A survey," *Automatica*, Vol. 49, No. 5, 2013, pp. 1087 – 1103. doi:https://doi.org/10.1016/j.automatica.2013.01.035, URL http://www.sciencedirect.com/science/article/pii/S0005109813000368.

[22] Bodson, M., "Evaluation of Optimization Methods for Control Allocation," *Journal of Guidance, Control, and Dynamics*, Vol. 25, No. 4, 2002.

[23] Agency, E. A. S., *Certification Specifications for Large Aeroplanes CS-25A19*, EASA, 2017.

[24] Jacobson, M., "Analyze N-dimensional Polyhedra in terms of Vertices or (In)Equalities," https://nl.mathworks.com/matlabcentral/fileexchange/30892-analyze-n-dimensional-polyhedra-in-terms-of-vertices-or-in-equalities, 2017.